Proc. 29th Int. Workshop on Vertex Detectors (VERTEX2020)
JPS Conf. Proc. **34**, 010009 (2021)
https://doi.org/10.7566/JPSCP.34.010009

Latest Developments and Results of Radiation Tolerance CMOS Sensors with Small Collection electrodes

I. Asensi Tortajada[1,2,*], P. Allport[3], M. Barbero[4], P. Barrillon[4], I. Berdalovic[1,5], C. Bespin[6], S. Bhat[4], D. Bortoletto[7], P. Breugnon[4], C. Buttar[8], R. Cardella[1], F. Dachs[1,13], V. Dao[1], Y. Degerli[12], H. Denizli[10], M. Dyndal[1], L. Flores Sanz de Acedo[1,8], P. Freeman[3], L. Gonella[3], A. Habib[4], T. Hemperek[6], T. Hirono[6], T. Kugathasan[1], I. Mandić[9], M. Mikuž[9], K. Moustakas[6], M. Munker[1], K.Y. Oyulmaz[10], P. Pangaud[4], H. Pernegger[1], F. Piro[1], P. Riedler[1], H. Sandaker[11], E.J. Schioppa[1], P. Schwemling[12], A. Sharma[1,7], L. Simon Argemi[8], C. Solans Sanchez[1], W. Snoeys[1], T. Suligoj[5], T. Wang[6], N. Wermes[6]

[1]*CERN* [2]*University of Valencia and Consejo Superior de Inv. Científicas (CSIC), Valencia, Spain* [3]*University of Birmingham, Birmingham, United Kingdom* [4]*Aix Marseille University, CNRS/IN2P3, CPPM, Marseille, France* [5]*University of Zagreb, Zagreb, Croatia* [6]*Rheinische Friedrich-Wilhelms Universität Bonn, Bonn, Germany* [7]*University of Oxford, Oxford, United Kingdom* [8]*University of Glasgow, Glasgow, United Kingdom* [9]*Jožef Stefan Institute, Ljubljana, Slovenia* [10]*Bolu Abant Izzet Baysal University, Bolu, Turkey* [11]*University of Oslo, Oslo, Norway* [12]*CEA-IRFU, Paris, France* [13]*Vienna University of Technology, Vienna, Austria*

E-mail: *ignacio.asensi@cern.ch

(Received December 9, 2020)

The development of radiation hard Depleted Monolithic Active Pixel Sensors (DMAPS) targets the replacement of hybrid pixel detectors to meet radiation hardness requirements of at least 1.5E16 1 MeV neq/cm2 for the HL-LHC and beyond.
DMAPS were designed and tested in the TJ180nm TowerJazz CMOS imaging technology with small electrodes pixel designs. This technology reduces costs and provides granularity of 36.4x36.4μm2 with low power operation (1 μW / pixel), low noise of ENC <20e$^-$, a small collection electrode (3 μm) and fast signal response within 25 ns bunch crossing.
This contribution will present the latest developments after the MALTA and Mini-MALTA sensors. It will illustrate the improvements and results of the Czochralski substrate with a bigger depletion zone to improve efficiency. It will also present the plans for MALTA2, which will be produced in late 2020, with enlarged transistors to reduce noise and cascoded front-end corrected slow control to improve chip operation.

KEYWORDS: Particle tracking detectors, Radiation-hard detectors, Electronic detector readout concepts, CMOS sensors, Monolithic active pixel sensors

1. Introduction

Recent prototypes with Depleted Monolithic Active Pixel Sensor (DMAPS) have been developed with the TowerJazz 180 nm CMOS imaging process to explore their viability for ATLAS [1] [2] [3] [4] [5], the High Luminosity LHC and for future HEP experiments. To be used in these experiments the efforts are focused in radiation hardness in order to meet requirements of up to 100 Mrad in Total Ionizing Dose (TID) and 10^{15} MeV n_{eq}/cm^2 and more.

The first two prototypes designed and issued were the large scale MALTA sensor [6] in January 2018, with a matrix of 512x512 and Mini-MALTA [7] in January 2019, a reduced-size prototype with a 16x64 pixel matrix. The pixel sensors presented on this paper have a small pixel size (36.4 x 36.4 μm2) and are produced on high resistivity epitaxial p-type silicon. They are characterized by a small

collection electrode of 3 μm diameter which results in small capacitance helping to minimize noise and achieve low power dissipation in the active area.

However, measurements in MALTA showed that after irradiation levels of 10^{15} MeV n_{eq}/cm^2, there is a loss in efficiency of the pixel corners because of the charge loss due to a low lateral electric field near the pixel borders. To improve detection efficiency after irradiation, special p-type and n-type implant geometries have been designed [8] and first used in Mini-MALTA and later in further implementations of MALTA.

This paper presents the latest developments and results after the MALTA and Mini-MALTA sensors. It will illustrate the improvements and results of the high resistivity Czochralski substrate with a bigger depletion zone to improve efficiency. And it will also present the plans for MALTA2, which has been recently submitted.

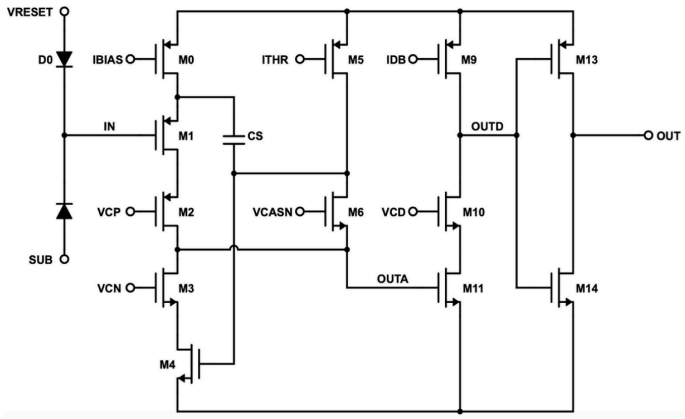

Fig. 1. MALTA and Mini-MALTA analog front-end

2. Evolution of MALTA and Mini-MALTA

The analog Front-end (FE) of MALTA and Mini-MALTA is shown in Fig. 1. Measurements on MALTA sensor revealed significant Random Telegraph Signal (RTS) noise, preventing lower threshold settings which was attributed to the ”M3” transistors being too small . To verify this assumption, the Mini-MALTA sensor includes sectors with the same ”M3” size as on MALTA and with a larger transistor. Measurements with Mini-MALTA confirmed that the RTS noise was decreased due to the larger transistor size, before and after irradiation.

Addressing the challenge of efficiency loss in the pixel corners after irradiation, the goal was to enlarge lateral electrical field to accelerate charge collection at the edge of the pixels. Fig. 2 shows the cross-section of the different process. On the top left it shows how detection efficiency is affected by diffusion. The others are the latest and different modifications of this process [9], which were optimized in TCAD simulations [8]. The top right shows the standard continuous n-layer. The bottom left shows adding a gap in the low dose n-layer through a mask change (n-gap). The bottom right shows the process of adding an extra deep p-type implant (p-well).

As shown in Fig. 3, the Mini-MALTA sensor, with 16×64 square pixels, has the matrix divided in 8 sectors with different pixel flavours, analog FE design, reset mechanism and electrode/well geometries. The left hand side has enlarged transistors to increase its gain and reduce the operational threshold [7]. The chip has an asynchronous read-out, with an improved slow-control with respect to MALTA and single serial data stream of 40Mbs or 1.2 Gpbs with 8b10b encoding. It operates with a

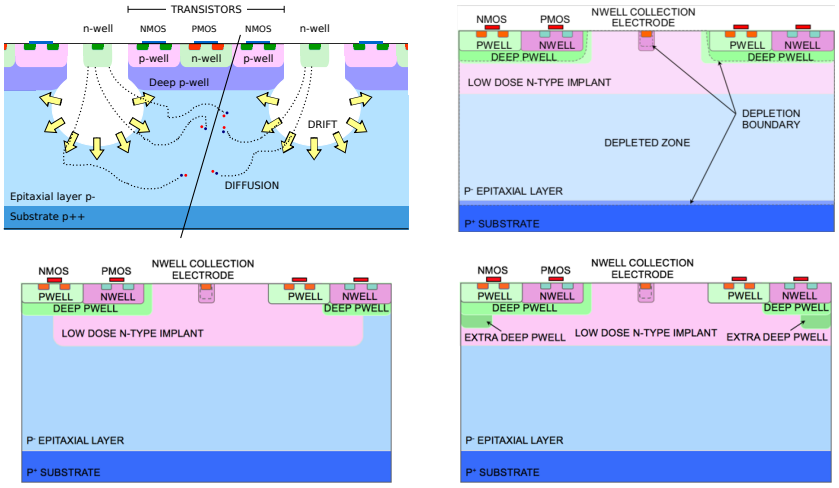

Fig. 2. TowerJazz process cross section. Top left: standard process. Top right: continuous n-layer. Bottom left: n-gap or low n-implant removed at the edged of the pixel. Bottom right: extra deep p-well at the edge of the pixel.

generated 600MHz clock generated with the provided external 40MHz clock.

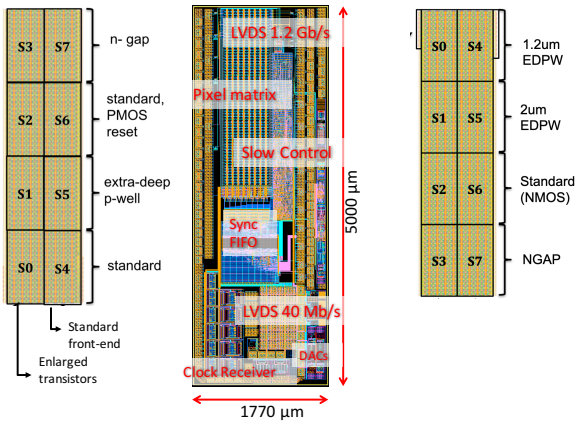

Fig. 3. Left: Mini-MALTA pixel groups. Center: Top view of Mini-MALTA. Right: Mini-MALTA with latest developments in front-end design.

A next version of Mini-MALTA with developments in the front-end was designed and produced, it has full cascoded front-end and enlarged ”M3” and ”M4” transistors. As seen in Fig. 3 on the right, changes were made in the pixel sectors: sectors 0 and 4 with 1.2µm extra deep p-well, 1 and 5 with 2µm extra deep p-well, 2 and 6 with standard n-layer and finally 3 and 7 with gap in n-layer.

MALTA C, a second version of MALTA was produced in August 2019 with the full size matrix and improved slow control. In order to increase the charge induced to the pixel, part of the samples were produced with Czochralski silicon wafers. Czochralski is the standard method to grow single crystalline silicon and it is only recently that it has become available with higher resistivity. The wafers used for the new production of the MALTA sensors are high-resistivity (>800 Ωcm) p-type Czochralski substrates which were thinned to 300 µm before measurements. The aim is improving radiation hardness with a thicker sensor in combination with small electrodes. MALTA Czochralski

has none of the modifications made to the Mini-MALTA transistors but some of the produced wafers have the continuous n-layer, deep p-well and n-gap designs.

MALTA 2, the successor of MALTA has been designed and submitted in October 2020. It has a matrix of 224x512 pixels of 36.4 µm size, with almost half size of MALTA, 20.2x10.1mm. The gain has been optimized to improve time resolution. It has a completely new slow control based on a 4322-bit shift register for easier operation. Part of the matrix has 2.4 larger "M3" and "M4" transistors with respect to enlarged transistors of Mini-MALTA. The full matrix has cascoded front-end for higher gain and reduced RTS noise, but with different gain values.

3. Measurements and results

3.1 Mini-MALTA

Fig. 4 shows the efficiency maps of a non-irradiated sensor on the left and after 1x10^{15} MeV n_{eq}/cm^2 irradiation on the right. The measurements were taken at -20°C and operated at -6V, with a low threshold of 200e$^-$ on sectors with enlarged transistors and 380e$^-$ for the standard size. White bins are noisy pixels on which efficiency has not been calculated. They are only present in the standard sectors.

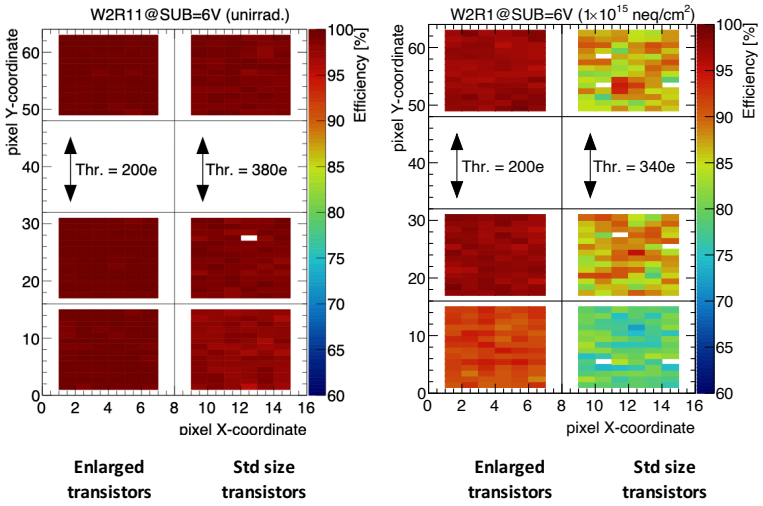

Fig. 4. Efficiency as a function for the track position. Left is nonirradiated, right after irradiation at 1x10^{15} MeV n_{eq}/cm^2

Before irradiation (left map), the average efficiency of enlarged transistors is 99.6±0.1%. On the sectors with standard transistors we can already observe lower efficiency: in the top 99.1±0.1% for the modification with gap in the n-layer, in the middle 98.9±0.1% for the extra deep p-well modification and in the bottom 97.9±0.1% for continuous n-layer.

On the right map shows the efficiency maps after 1x10^{15} MeV n_{eq}/cm^2 neutron irradiation. Sensor regions with enlarged transistors (on the left) have lower decrease of average efficiency with respect to standard transistors: 91.9% in the region with continuous n-layer, 97.9% with extra deep p-well and 97.6% with n-gap modification. There is higher decrease in efficiency, which is still observed in the regions around the pixel corners, in standard transistors regions due to the lower gain and high threshold (380e$^-$) regardless of the modifications. Efficiencies are: 78.8% in the continuous n-layer, 87.0% in extra deep p-well and 86.5% in n-gap modification.

Clearly enlarged transistors significantly increase efficiency for sensors after irradiation due to the higher gain, lower gain spread and reduced RTS noise with also the absence of noisy pixels.

Measurements at Diamond [10] show the photon pixel response as function of dose. To calculate the response, the average number of hits was calculated in a small region around the pixel centre. Then, the number of hits in each pixel, calculated within a 36.4×36.4 μm^2 square, was normalised to that average. This average is defined as the relative photon pixel response. At the pixel edges, charge can be picked up by two pixels at the same time, which leads to a response above 1.

As Fig. 5 shows, before irradiation almost all of the pixel is fully responsive, except for the corners specially in the continuous n-layer modification and around the edges. After irradiation the decrease of response in the corner and around the edges is around 10% in continuous n-layer and almost no reduction on extra deep p-well and n-gap modifications which is in line with the TCAD simulations [8].

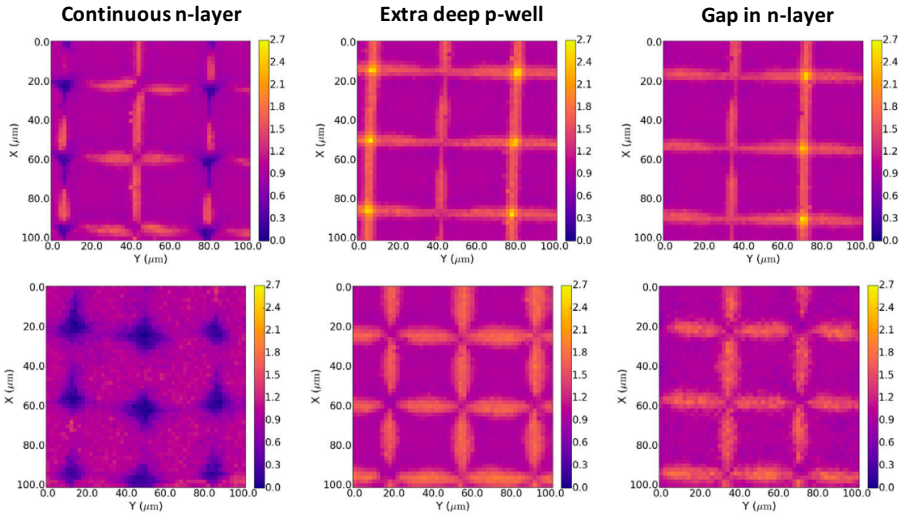

Fig. 5. Mini-MALTA pixel response maps for the different samples and modifications. On the top W2R11 is unirradiated, on the bottom W2R1 is neutron-irradiated to 1e10^{15} MeV n_{eq}/cm^2.

The performance of the different pixel configurations can be further studied by the effect of the threshold in the efficiency. The enlarged size of the NMOS transistor "M3" allows using a lower threshold to achieve higher efficiency. Furthermore, extra deep p-well and gap in n-layer modifications improve charge collection and show higher efficiency as seen in Fig. 6 in two sensors after being irradiated with 1e10^{15} MeV n_{eq}/cm^2. Able to operate at a lower threshold with large transistors, efficiency is achieved at almost 95% in the continuous n-layer sectors, 98% with the n-gap and 99% with extra deep p-well. Standard transistors perform lower efficiency at higher thresholds, around 88% with the extra deep p-well and n-gap modifications and less than 80% with standard transistors. These results highlight the importance of the "M3" transistor enlargement and the lower performance of the continuous n-layer modification with respect to n-gap and extra deep p-well. It has also being measured after 2x10^{15} MeV n_{eq}/cm^2 irradiation efficiency remaining above 90% in sectors with enlarged transistors.

Radiation hardness after 100Mrad of Total Ionizing Dose (TID) is shown in Fig. 7. On the left there is the Equivalent Noise Charge (ENC) as function of TID. We can observe an increase from an initial noise of 10e$^-$ in all sectors to 20e$^-$ in sectors with enlarged transistors and up to 27e$^-$ in the MALTA standard sectors. On the right it is measured the iron X-ray signal amplitude as function of TID. There is a constant higher gain in enlarged transistors than with standard.

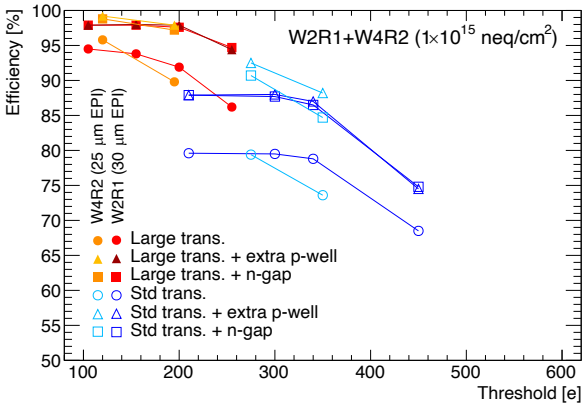

Fig. 6. Efficiency as a function of threshold for two different Mini-MALTA samples. Neutron irradiated to 1e15^{15} MeV n_{eq}/cm^2, and measured with 2 GeV electron beam at ELSA, with 6 V bias voltage

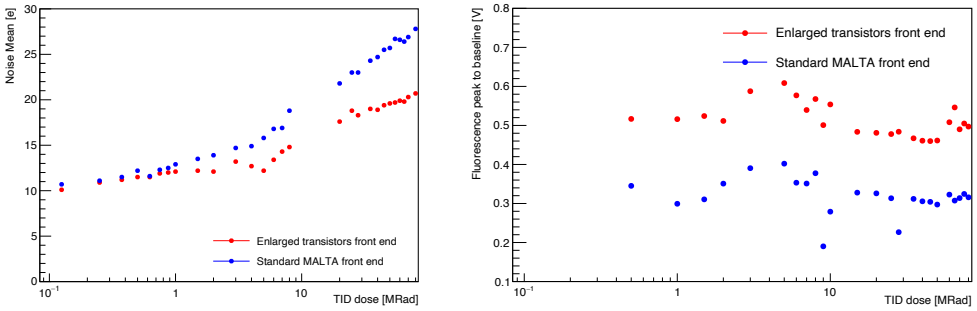

Fig. 7. Mini-MALTA measurements. Left: ENC noise as function of total ionising dose (TID). Right: Signal gain for Fe-target fluorescence X-ray as function of TID.

3.2 MALTA Czochralski (Cz)

Using the high-resistivity Czochralski substrate requires that the substrate can be biased at higher voltage to accomplish full depletion of the substrate.

Operational limits have been studied measuring current in p-well and SUB as function of SUB voltage. Limits are affected by punch-trough current that can flow between substrate and p-well and by leakage current flowing from substrate and p-well to the collection electrode. Measurement shown in Fig. 8 shows how operation at -50V is reached without punch-through between the deep p-well and the p-type Cz substrate through the n-layer.

Fig. 9 shows the highly improved radiation hardness of the new MALTA Cz due to the higher signal amplitude generated in larger depletion zone in high-resistivity substrate [11]. On the left, before irradiation there is a efficiency of 98.5% with 424e$^-$ threshold. On the center, after 1x10^{15} MeV n_{eq}/cm^2 of neutron irradiation an efficiency of 97.0% is measured in a n-gap region with 260e$^-$ threshold. On the right, after 2x10^{15} MeV n_{eq}/cm^2 of neutron irradiation an efficiency of 95.4% is measured in a n-gap region with 226e$^-$ threshold. These results can be compared with the lower efficiency of the Mini-MALTA standard transistor sectors in Fig. 4 after irradiation.

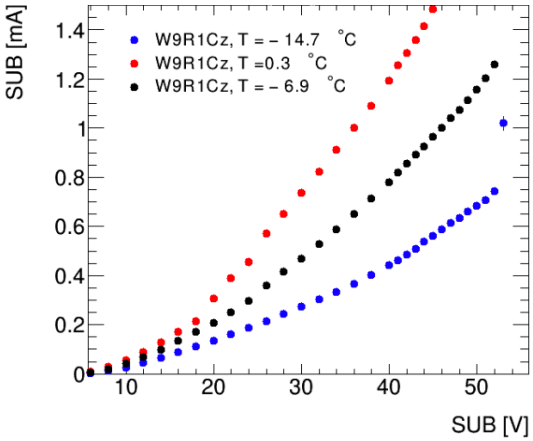

Fig. 8. MALTA Czochralski higher operation voltage. Current as a function of bias voltage.

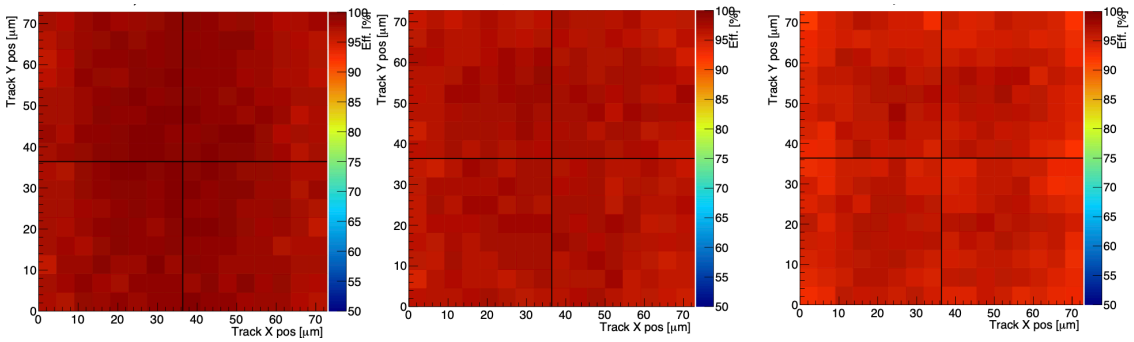

Fig. 9. MALTA with Czochralski efficiency maps. Left: Continuous n-layer before irradiation. Center: n-gap after 10^{15} MeV n_{eq}/cm^2. Right: n-gap after 2x10^{15} MeV n_{eq}/cm^2

4. Conclusions

Latest developments in the RnD of Depleted Monolithic Active Pixel Sensors show significant improvements in radiation hardness with the aim of upgrade of tracking detectors for the HL-LHC and beyond. The MALTA and Mini-MALTA sensors and their following versions including the ones with Czochralski substrate have made significant steps in the need of fast and radiation hard CMOS sensors.

Mini-MALTA sensor with pixel and process modifications of extra deep p-well and gap in n-layer has measured full radiation hardness after 10^{15} MeV n_{eq}/cm^2 and 100Mrad. The charge loss at the corners have been reduced with a more directive electrical field to the collection electrode.

The usage of high-resistivity Czochralski substrate has demonstrated a full efficiency after 10^{15} MeV n_{eq}/cm^2 and it is promising beyond. All the knowledge acquired with the previous experience has been applied to the design and recent submission of MALTA 2.

References

[1] ATLAS collaboration, Technical Design Report for the ATLAS Inner Tracker Pixel Detector, Tech. Rep. CERN-LHCC-2017-021. ATLAS-TDR-030, 2017.
[2] G. Aglieri, et al., Monolithic active pixel sensor development for the upgrade of the inner tracking system of the ALICE experiment at CERN, J. Instrum. 8 (2013) C12041.
[3] Berdalovic I., et al. CMOS Pixel development in towerjazz 180 nm CMOS for the outer pixel layers in

the ATLAS experiment J. Instrum., 13 (2018), Article C01023 11th International Conference on Position Sensitive Detectors, 3–8, 2017

[4] Wang T., et al. Depleted fully monolithic CMOS pixel detectors using a column based readout architecture for the ATLAS inner tracker upgrade J. Instrum., 13 (2018), p. C03039

[5] Moustakas K., et al. Development in a novel CMOS process for depleted monolithic active pixel sensors NSS-MIC 2017 Conference Record 978-1-5386-2282-7/17, IEEE (2017)

[6] R. Cardella, et al., MALTA: an asynchronous readout CMOS monolithic pixel detector for the ATLAS high-luminosity upgrade, J. Instrum. 14 (2019) C06019.

[7] M. Dyndal, et al., Mini-MALTA: Radiation hard pixel designs for small-electrode monolithic CMOS sensors for the High Luminosity LHC, J. Instrum. 15 (2020) P02005.

[8] M. Munker, M. Benoit, D. Dannheim, A. Fenigstein, T. Kugathasan, T. Leitner, et al., Simulations of CMOS pixel sensors with a small collection electrode, improved for a faster charge collection and increased radiation tolerance, J. Instrum. 14 (2019) C05013, arXiv:1903.10190.

[9] W. Snoeys, et al., A process modification for CMOS monolithic active pixel sensors for enhanced depletion, timing performance and radiation tolerance, Nucl. Instrum. Methods A 871 (2017) 90–96.

[10] M. Mironova, Metodiev, Allport, I. Berdalovic, D. Bortoletto, Buttar, Cardella et al., Measurement of the relative response of small-electrode CMOS sensors at Diamond Light Source, J. Nuclear Instruments and Methods in Physics Research,956 (2020)

[11] H. Pernegger, et al., First tests of a novel radiation hard cmos sensor process for depleted monolithic active pixel sensors, J. Instrum. 12 (2017) P06008.